Globally Downscaled Climate Projections for Assessing the Conservation Impacts of Climate Change

2 authors:

Karyn Tabor
Conservation International
7 PUBLICATIONS   **182** CITATIONS

John W Williams
University of Wisconsin–Madison
145 PUBLICATIONS   **6,877** CITATIONS

Globally downscaled climate projections for assessing the conservation impacts of climate change

Karyn Tabor[1,3] and John W. Williams[2]

[1]*Center for Applied Biodiversity Science (CABS), Conservation International, 2011 Crystal Drive, Suite 500, Arlington, Virginia 22202 USA*
[2]*University of Wisconsin, Department of Geography, Center for Climatic Research, Land Tenure Center, 550 North Park Street, University of Wisconsin, Madison, Wisconsin 53706 USA*

Abstract. Assessing the potential impacts of 21st-century climate change on species distributions and ecological processes requires climate scenarios with sufficient spatial resolution to represent the varying effects of climate change across heterogeneous physical, biological, and cultural landscapes. Unfortunately, the native resolutions of global climate models (usually approximately $2° \times 2°$ or coarser) are inadequate for modeling future changes in, e.g., biodiversity, species distributions, crop yields, and water resources. Also, 21st-century climate projections must be debiased prior to use, i.e., corrected for systematic offsets between modeled representations and observations of present climates. We have downscaled future temperature and precipitation projections from the World Climate Research Programme's (WCRP's) CMIP3 multi-model data set to 10-minute resolution and debiased these simulations using the change-factor approach and observational data from the Climatic Research Unit (CRU). These downscaled data sets are available online and include monthly mean temperatures and precipitation for 2041–2060 and 2081–2100, for 24 climate models and the A1B, A2, and B1 emission scenarios. This paper describes the downscaling method and compares the downscaled and native-resolution simulations. Sharp differences between the original and downscaled data sets are apparent at regional to continental scales, particularly for temperature in mountainous areas and in areas with substantial differences between observed and simulated 20th-century climatologies. Although these data sets in principle could be downscaled further, a key practical limitation is the density of observational networks, particularly for precipitation-related variables in tropical mountainous regions. These downscaled data sets can be used for a variety of climate-impact assessments, including assessments of 21st-century climate-change impacts on biodiversity and species distributions.

Key words: biodiversity impacts; climate projections; downscaling; global climate models; IPCC scenarios; species distributions.

Introduction

Twenty-first-century climate scenarios from general circulation models (GCMs) are essential for assessing the potential responses of ecological, physical, and cultural systems to climate change. Climate is a critical control on species distributions, and there is a rich literature on using climate simulations and species distributional models to predict extinction risk, set conservation priorities, and assess species range shifts under various 21st-century climate scenarios (e.g., Malcolm et al. 2002, Pearson and Dawson 2003, Thomas et al. 2004, Thuiller et al. 2005, Morin and Lechowicz 2008). However, the coarse resolution of most GCMs (grid cell sizes typically ranging from 1° to 5°, and a typical resolution of about 2.8°; Randall et al. 2007) is insufficient for detailed assessment of land-surface processes and climate-change impacts at local to regional scales, especially in regions with heterogeneous land cover and diverse topography (Wilby et al. 1998, 2004). For example, finer-resolution climate grids are necessary for ecosystem models (Zhang 2006), soil-erosion models (Zhang 2006), and hydrological models (Fowler et al. 2007) where sub-degree resolution is required to simulate stream flow in mountainous catchments (Salathé et al. 2007). Species distribution models also require high-resolution data sets (Kremen et al. 2008) to set conservation priorities for habitats and species under various future climate scenarios. In many cases the species that are most vulnerable to climate change are already confined to small habitats (Kremen et al. 2008). Furthermore, protected-area planning must occur on a fine scale, because 75% of globally recognized protected parks and reserves are <300 km² in area (WDPA 2006). Thus, there is an urgent demand for high-resolution future-climate scenarios, which can be met by downscaling GCM simulations.

Another challenge for ecologists and conservation biologists wishing to explore how climate change will affect species distributions and ecological processes is

that GCM simulations will always differ somewhat from observed reality, a phenomenon known as model bias. Simply comparing a 21st century simulation to present observed climates is inappropriate because such a comparison aggregates both the simulated change in 21st-century climates (due to changes in greenhouse gases and other radiative forcings) with the artifactual difference between present-day simulated and observed climates. For example, if the simulated global mean temperatures for the late 20th century were 2°C colder than those actually observed, a 5°C simulated warming by AD 2100 would only appear as a 3°C warming compared to modern observations. Thus, downscaling techniques must also attempt to debias the simulated climatologies. It is impossible to know whether model bias has been completely removed, but it can at least be minimized by the appropriate debiasing technique.

Downscaling techniques include dynamic downscaling, statistical downscaling, and the change-factor method. Each methodology has its advantages and limitations. *Dynamic downscaling* embeds regional climate models (RCMs) within large-scale GCMs. RCMs explicitly represent atmospheric processes operating at sub-grid scales for GCMs, such as orographic rainfall and surface–atmosphere interactions (Fowler et al. 2007). However, RCMs are computationally expensive because they must numerically solve many thermodynamic equations describing, e.g., the atmospheric state of motion, the passage of radiation through the atmospheric, cloud formation and other hydrological process, and surface–atmosphere interactions, all at a short time step (~30 minutes), at a high spatial resolution, and across multiple layers of the atmosphere (Díez et al. 2005, Spak et al. 2007). Consequently, for many regions only a limited number of RCM simulations currently are available, which prevents a good characterization of the uncertainty of climate projections given their sensitivity to different climate-model parameters (Diffenbaugh et al. 2008).

Statistical downscaling assumes that regional climates are affected by both large-scale atmospheric processes and regional forcings (Wilby et al. 2004, Hewitson and Crane 2006). The statistical relationships between large-scale climate variables, such as atmospheric pressure fields, and local variables, such as rainfall, are determined from observational data and then applied to the GCM simulations to project regional-scale climate changes (Wilby et al. 2004). The advantage of this approach is that it uses relatively robust large-scale features of the GCM simulations as predictors for the local variables. Because the relationships between large-scale and local variables vary by landscape, most statistical downscaling studies are limited to individual regions (Hayhoe et al. 2004, Shongwe et al. 2006, Benestad et al. 2007, Spak et al. 2007). Another disadvantage of this technique is that it assumes that the relationship between large-scale processes and local variables is stationary over time.

The *change-factor technique* is the simplest and fastest of the three techniques for processing numerous data sets with large spatial extents, making it by far the most feasible approach for global-scale downscaling of a large number of climate simulations (Wilby et al. 2004). This method has been widely employed in climate change research, e.g., generating future climate scenarios for high-resolution modeling of vegetation and ecological sensitivity to climate change in the United States, Vegetation/Ecosystem Modeling and Analysis Project (VEMAP; Kittel et al. 1995), and projecting shifts in mediterranean climates (Klausmeyer and Shaw 2009). In the change-factor method, the climate variables of interest are directly downscaled from the GCM's native resolution to the resolution of a target high-resolution observational data set. First, the simulated "present" values for a variable (e.g., monthly mean temperature for 1961–1990) are subtracted from the future values simulated by the same GCM (Wilby et al. 2004, Klausmeyer and Shaw 2009). The resulting differences, referred to as "climate anomalies," are then resampled to the desired resolution of the observational data set using standard spatial interpolation techniques (e.g., bilinear or thin-spline interpolation). The interpolated anomalies are then added to the target fine-resolution observational data set covering the same time period as the present GCM simulation. The resulting downscaled and debiased future-climate projections have two advantages over the original GCM simulations: (1) the high-resolution observational data set already incorporates local-scale to regional-scale climatic processes (e.g., local orographic effects on temperature and precipitation), and (2) the differencing procedure minimizes any persistent systematic biases between observed and simulated 20th-century climates. Just as with statistical downscaling, the change-factor technique assumes that the relationship between large-scale processes and local variables is stationary over time, and further assumes that the difference between model simulations and "true" climates is stationary over time (Diaz-Nieto and Wilby 2005).

The validity of the assumptions contained in the statistical downscaling and change-factor techniques is debatable, particularly for the large climate changes projected for the 21st century. Even regional climate modeling is hardly assumption-free, although these assumptions are more grounded in mechanistic rather than statistical descriptions of climate processes. Thus, the three downscaling techniques outlined above roughly fall along a continuum ranging from approaches that are more expensive computationally but perhaps contain fewer assumptions, to those that are less expensive but are based on a weaker set of assumptions. All three techniques are used in the climatological literature, and the choice of technique depends on the need for low-cost approaches (which permit many simulations to be downscaled globally) vs. more climatologically rigorous approaches.

Given the immediate and urgent need for scale-appropriate climate-impact assessments in conservation biology and other disciplines, we have implemented the change-factor approach as a computationally efficient means of downscaling the many climate simulations for the 21st century from the Intergovernmental Panel on Climate Change Fourth Assessment Report (IPCC AR4) (IPCC 2007). All models are downscaled to a 10-minute spatial resolution (~17-km resolution at the equator). The great advantage to downscaling multiple models is the ability to produce multi-model "ensembles" or multi-model means that help minimize and/or assess uncertainties associated with individual model biases or errors (Meehl et al. 2007b, Randall et al. 2007, Diffenbaugh et al. 2008, Giorgi and Diffenbaugh 2008). In this paper, we describe the methods used to create the 10-minute downscaled and debiased climate projections, present representative visualizations of climate variables, discuss uncertainties in the resultant downscaled climate projections, and explain how downscaled climate projections enhance species range modeling. This global data set is publicly *available online*.[4] It will be a valuable resource for conservation biologists and others assessing the impacts of 21st-century climate change. By providing downscaled results for the complete set of 21st-century climate scenarios from IPPC AR4, we improve the capacity of conservation biologists to generate robust projections of species responses to climate change (Araújo and Guisan 2006).

MATERIALS AND METHODS

Overview

We downscaled the climate simulations for future-emissions scenarios A1B, A2, and B1, for 24 coupled atmosphere–ocean global circulation models (AOGCMs) obtained from the World Climate Research Programme's (WCRP's) Coupled Model Intercomparison Project phase 3 (CMIP3) multi-model data set (Meehl et al. 2007a). Twenty-three of these AOGCMs are evaluated in the IPCC AR4 (Intergovernmental Panel on Climate Change Fourth Assessment Report; IPCC 2007). All climate simulations were regridded to a 10-minute resolution and debiased to correct for systematic differences between simulated and observed climates for the late 20th century. Regridded monthly temperature and precipitation means are provided for two time windows, representing the middle and end of the 21st century. We use the Climatic Research Unit (CRU) CL 2.0 10-minute data set (New et al. 2002) as our baseline modern observational data set. All downscaled data sets are available online (see footnote 4).

IPCC emissions scenarios

The three 21st-century standard emissions scenarios analyzed here (A2, A1B, and B1) represent a range of the possible future scenarios explored by the IPCC (Nakicenovic and Swart 2000, Meehl et al. 2007b), with no explicit probability attached to any. The B1 scenario assumes the most ecologically friendly future world where economies are less energy intensive and shift towards technological development and sharing of non-carbon-intensive energy sources. The A1B scenario assumes that future energy sources will be balanced between fossil-intensive and non-fossil energy sources. The A2 scenario is characterized by slow and regionalized development of resource-efficient technologies, therefore globally still heavily dependent on fossil-fuel consumption. These three scenarios result in substantially different atmospheric concentrations of CO_2 and other long-lived greenhouse gases by the end of this century (Meehl et al. 2007b). Future CO_2 concentrations are highest in the A2 scenario, reaching 856 ppm by 2100 and with an accelerating rate of growth at the end of the century. In the A1B scenario, CO_2 concentrations reach 717 ppm by 2100 and continue to increase at the end of the century. In the B1 scenario, CO_2 concentrations reach 549 ppm by the end of the century, and are nearly stabilized (Nakicenovic and Swart 2000).

Downscaling

The change-factor downscaling procedure requires two primary inputs, the AOGCM climate simulations and the 20th-century observed data sets (Fig. 1). First, we downloaded the monthly means of air temperature (temperature) and precipitation flux (precipitation) for the 20th and 21st centuries (Fig. 1, Inputs) from the CMIP3 multi-model data set available online through the University Corporation for Atmospheric Research's (UCAR) Earth System Grid (UCAR 2002). One simulation from each model (20c3m) was used to represent simulated 20th-century climates and three scenarios (A1B, A2, and B1) were used to represent possible 21st-century climate trajectories. Table 1 shows the names of all AOGCMs and scenarios downscaled here along with their original spatial resolutions. In processing step I (Fig. 1), we used the MexNC toolbox for netCDF files (Evans 2008) for Matlab (MATLAB 2007) to extract monthly surface temperature and precipitation variables from the netCDF formatted data files, used by WCRP CMIP3, for three time periods: AD 1961–1990 (referred to as the late-20th-century or the 1975 mean), AD 2041–2060 (middle-21st-century or 2050 mean), and AD 2081–2100 (late-21st-century or 2090 mean). For each period, we calculated the climatologic means and interannual variability (standard deviations) for monthly temperature and precipitation. The second primary input (Fig. 1) was the observed late-20th-century monthly temperatures and precipitation from Climatic Research Unit (CRU) CL 2.0 (*available online*),[5] at 10-minute resolution (New
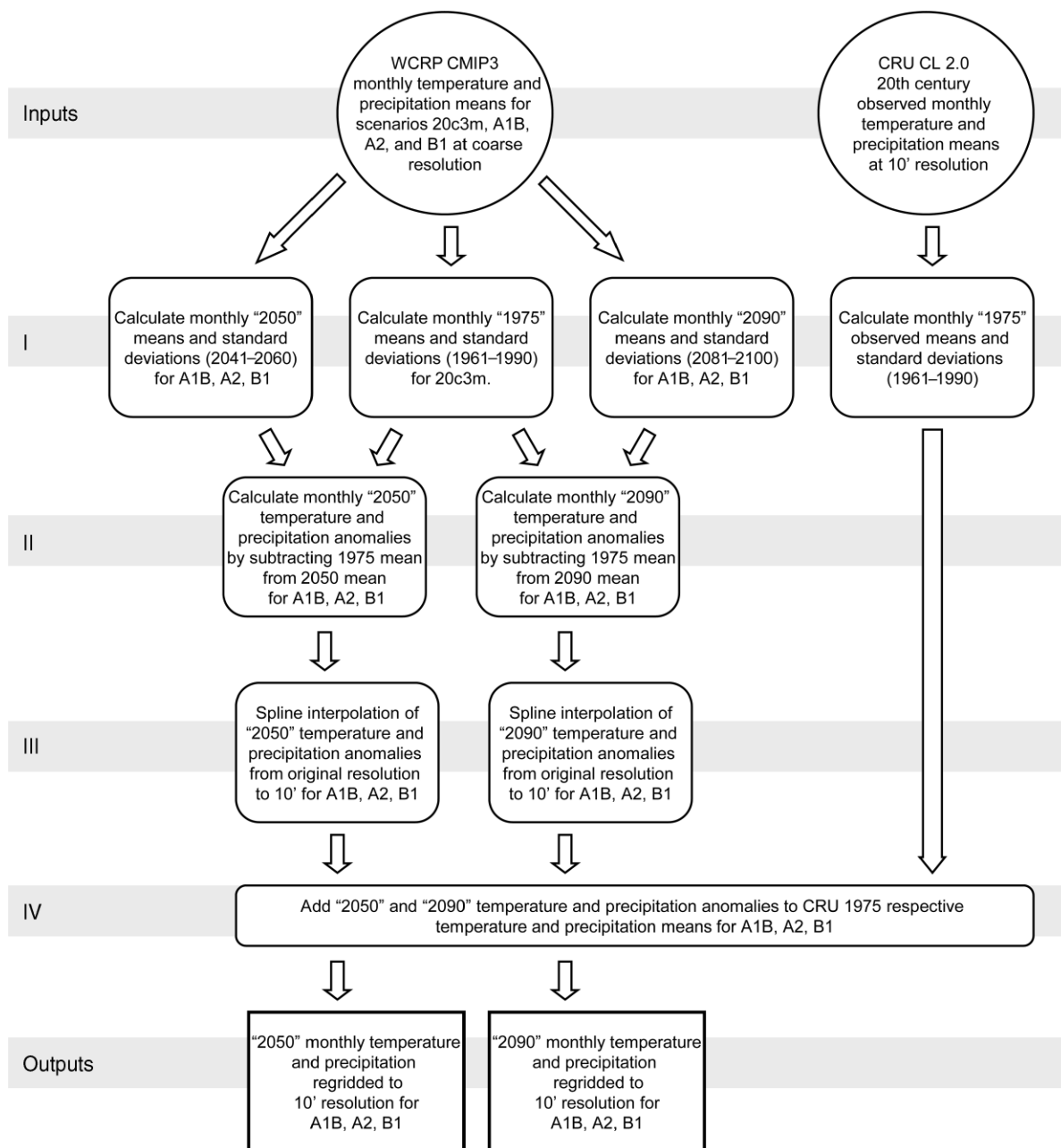
FIG. 1. A flowchart illustrating the downscaling procedure beginning with the original data from the CMIP3 multi-model data set and ending with 10-minute resolution downscaled climatologies for AD 2050 and 2090. Roman numerals at left indicate the four major processing steps. Scenario 20c3m is the historical 20th-century model run for the AOGCMs, while scenarios A1B, A2, and B1 are future-emission scenarios (described in *Materials and methods: IPCC emission scenarios*).

et al. 2002). Late-20th-century monthly means and standard deviations also were calculated for the CRU observations (AD 1961–1990).

We debiased the AOGCM climate projections by adding the simulated changes of the 21st century, expressed relative to the baseline simulation, to current observed climates. To do this, we calculated climate anomalies by subtracting the 1975 means for precipitation and temperature from the 2050 and 2090 means at

the native AOGCM resolution (Fig. 1, Step II). These 2090–1975 and 2050–1975 anomalies were regridded to a 10-minute resolution using a cubic spline interpolation (Step III), then added to the observed CRU monthly temperature and precipitation means for 1961–1990 (Step IV). This procedure is repeated for each combination of AOGCM and emissions scenario listed in Table 1. Spline interpolations were performed with Matlab's interp3 function and its "spline" setting, which

TABLE 1. The 24 CMIP3 archive global climate models (atmosphere–ocean general circulation models [AOGCMs]) we downscaled to 10-minute resolution (arranged alphabetically by model).

Source	Country	Model	Resolution		Scenario		
			y	x	A1B	A2	B1
Bjerknes Centre for Climate Research	Norway	BCCR-BCM2.0	2.80	2.80	X	X	X
National Center for Atmospheric Research	USA	CCSM3	1.41	1.41	X	X	X
Canadian Centre for Climate Modelling	Canada	CGCM3.1(T47)	3.75	3.75	X	X	X
and Analysis		CGCM3.1(T63)	2.80	2.80	X		X
Centre National de Recherches Météorologiques, Météo-France	France	CNRM-CM3	2.80	2.80	X	X	X
Commonwealth Scientific and Industrial	Australia	CSIRO-MK3.0	1.90	1.90	X	X	X
Research Organisation (CSIRO) Atmospheric Research		CSIRO-MK3.5	1.90	1.90	X	X	X
Max Planck Institute for Meteorology	Germany	ECHAM5/MPI-OM	1.90	1.90	X	X	X
Meteorological Institute of the University of Bonn, Meteorological Research Institute of the Korea Meteorological Administration (KMA), and Model and Data Group	Germany and Korea	ECHO-G	3.90	3.90	X	X	X
National Key Laboratory of Numerical Modeling for Atmospheric Sciences and Geophysical Fluid Dynamics (LASG), Institute of Atmospheric Physics	China	FGOALS-g1.0	2.80	2.80	X		X
Geophysical Fluid Dynamics Laboratory	USA	GFDL-CM2.0	2.00	2.50	X	X	X
(GFDL), National Oceanic and Atmospheric, Administration (NOAA), U.S. Department of Commerce		GFDL-CM2.1	2.00	2.50	X	X	X
Goddard Institute for Space Studies (GISS),	USA	GISS-AOM	3.00	4.00	X		X
National Aeronautics and Space		GISS-EH	4.00	5.00	X		
Administration (NASA)		GISS-ER	4.00	5.00	X	X	X
National Institute of Geophysics and Volcanology (INGV)	Italy	INGV-SXG	1.13	1.13	X	X	
Institute for Numerical Mathematics	Russia	INM-CM3.0	4.00	5.00	X	X	X
Institut Pierre Simon Laplace	France	IPSL-CM4	2.50	3.75	X	X	X
Center for Climate System Research (University	Japan	MIROC3.2 (high resolution)	1.10	1.10	X		X
of Tokyo), National Institute for Environmental Studies, and Frontier Research Center for Global Change		MIROC3.2 (medium resolution)	2.80	2.80	X	X	X
Meteorological Research Institute	Japan	MRI-CGCM2.3.2	2.80	2.80	X	X	X
National Center for Atmospheric Research	USA	PCM	2.80	2.80	X	X	X
Hadley Centre for Climate Prediction	UK	UKMO-HadCM3	2.50	3.75	X	X	X
		UKMO-HadGEM1	1.30	1.90	X	X	

Note: The table details model sources, native resolutions (Randall et al. 2007), and model availability for emission scenarios A1B, A2, and B1 (Meehl et al. 2007*a*), with availability indicated by the presence of an "X."

constructs a smooth interpolated curve from a series of piecewise third-order polynomials (de Boor 1978). Because the CRU data set covers global land areas only, the regridded 21st-century climatologies presented here are also only for land areas.

RESULTS

To illustrate how the debiasing procedure works, we show the original and downscaled results for South America for January and July, for temperature (Fig. 2) and precipitation (Fig. 3), using simulations from the A1B scenario of the GISS-ER model. For January temperature (Fig. 2: top half), one of the most obvious discrepancies between late-20th-century observations and simulations is the concentration of higher-than-observed temperatures in south-central South America, covering eastern Bolivia, all of Paraguay and northern Argentina. If, as is likely, this too-warm bias between the present simulated and observed temperatures persists in the 21st-century climate simulations, then naïve

use of the 21st-century simulations (i.e., without any attempt to correct for the too-warm bias) would result in warm temperature projections and too-severe assessments of climate-change impacts in this region. This bias is apparent also in the 2090 uncorrected simulations, but is removed from the 10-minute debiased and downscaled 2090 temperature maps for South America (Fig. 2: top half). For July temperature (Fig. 2: bottom half), no major discrepancies between the late-20th-century observations and simulations are apparent, except where the fine-scale features of the Andes Mountains are smoothed over in the 3° × 3° maps. Similar kinds of discrepancies between observation and reality can be found for any climate-model simulation, for various regions of the world. Model bias is a general phenomenon and the example of GISS-ER for South America is only chosen for illustration.

As another example, January precipitation maps (Fig. 3: top half) show a large discrepancy in south-central South America between simulated and observed late-
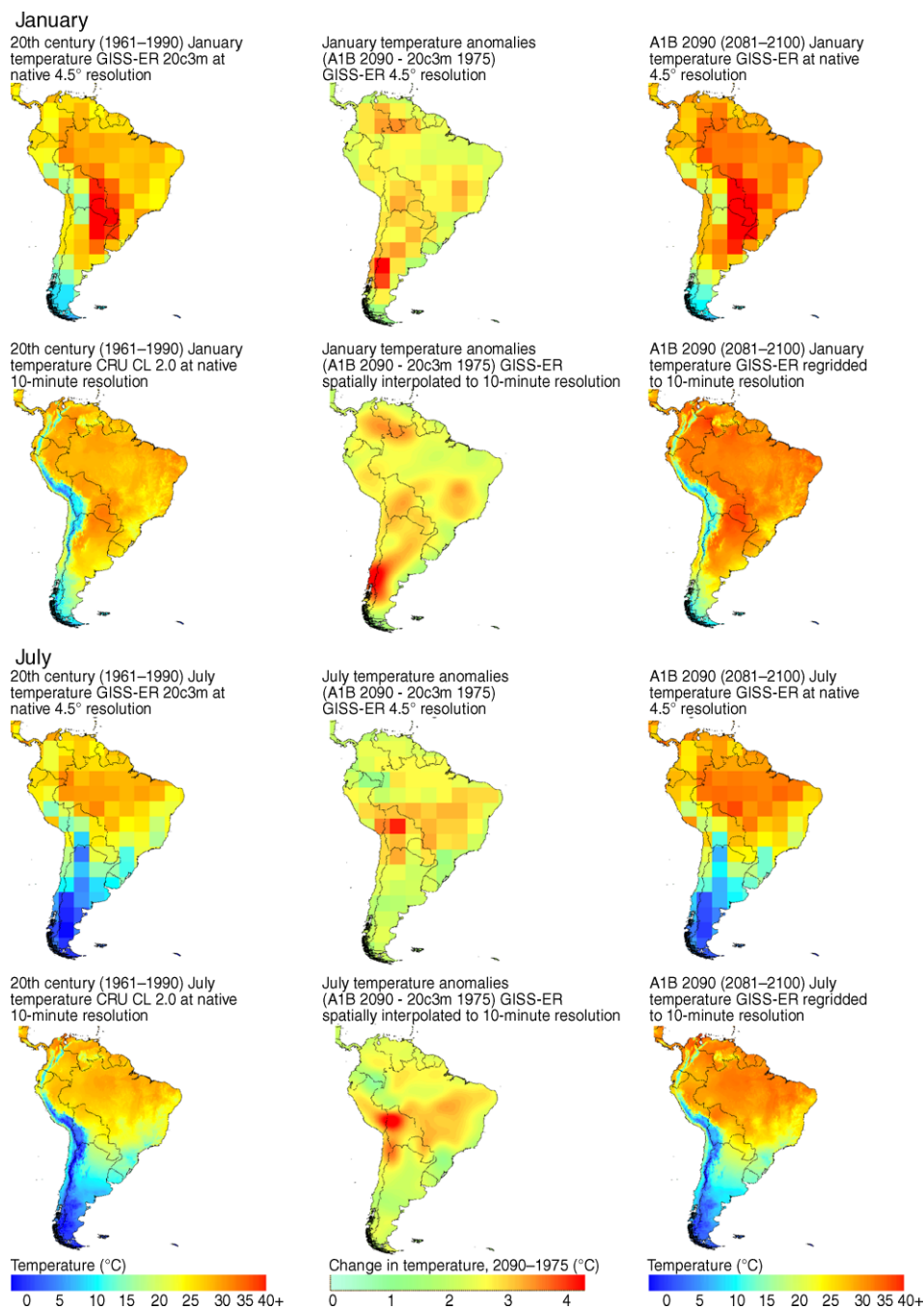
FIG. 2.   South American 2090 temperature estimates from NASA's GISS-ER model and the A1B scenario, at the original GCM resolution of 4.5° (left column) and the downscaled 10-minute resolution (right column) for January (top two rows) and July (bottom two rows). The middle column shows the temperature anomaly calculated by subtracting the simulated late-20th-century temperature from the late-21st-century simulated temperature (Fig. 1, step II). The temperature anomaly is shown at the original 4.5° resolution and the interpolated 10-minute resolution.

20th-century values, with simulated precipitation much lower than observations. Additionally, there is a significant difference in January rainfall in eastern in Brazil, where CRU observations are almost 200 mm less than simulated precipitation. For July precipitation (Fig. 3: bottom half), the most obvious discrepancy occurs over Uruguay and southeast Brazil where the CRU observed data is over 100 mm wetter than simulated precipitation. Again, these sorts of discrepancies are not confined to GISS-ER and South America.

Globally, the regridded climate projections show broad similarities to the original AOGCM simulations,

January

20th century (1961–1990) January
precipitation GISS-ER 20c3m at
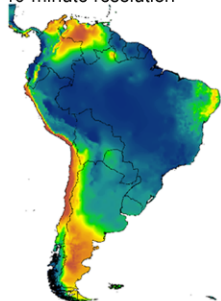native 4.5° resolution
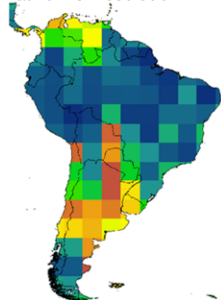
January precipitation anomalies
(A1B 2090 - 20c3m 1975)
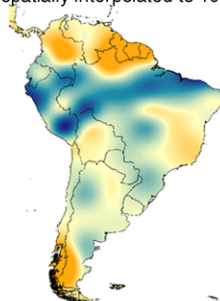GISS-ER 4.5° resolution
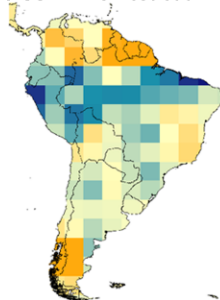
A1B 2090 (2081–2100) January
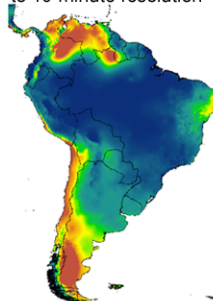precipitation GISS-ER at native
4.5° resolution
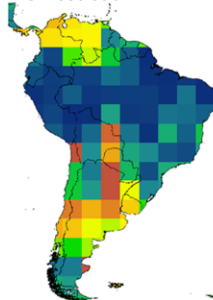
20th century (1961–1990) January
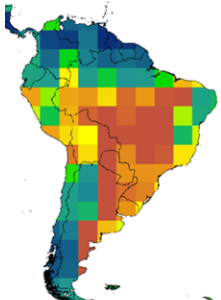precipitation CRU CL 2.0 at native
10-minute resolution

January precipitation anomalies
(A1B 2090 - 20c3m 1975) GISS-ER
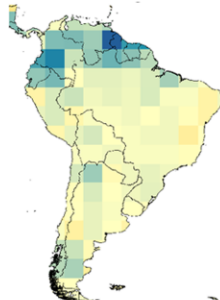spatially interpolated to 10-minute resolution

A1B 2090 (2081–2100) January
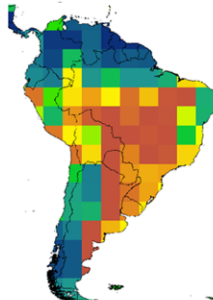precipitation GISS-ER regridded
to 10-minute resolution

July

20th century (1961–1990) July
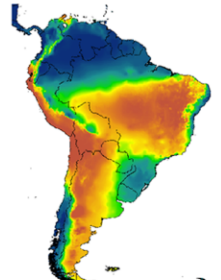precipitation GISS-ER 20c3m at
native 4.5° resolution

July precipitation anomalies
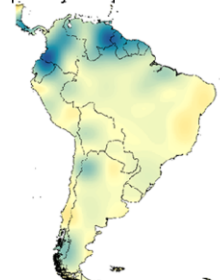(A1B 2090 - 20c3m 1975)
GISS-ER 4.5° resolution

A1B 2090 (2081–2100) July
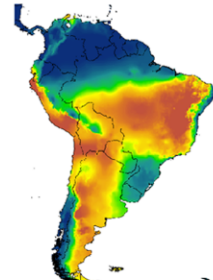precipitation GISS-ER at native
4.5° resolution

20th century (1961–1990) July
precipitation CRU CL 2.0 at native
10-minute resolution

July precipitation anomalies
(A1B 2090 - 20c3m 1975) GISS-ER
spatially interpolated to 10-minute resolution

A1B 2090 (2081–2100) July
precipitation GISS-ER regridded
to 10-minute resolution

Precipitation (mm)

0   20   40   60   100 200 400+

Change in precipitation, 2090–1975 (mm)

−60 −20 −5   0   80 40   80   100   120+

Precipitation (mm)
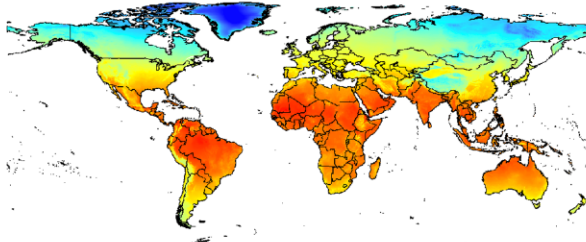
0   20   40   60   100 200 400+

Fig. 3.   South American 2009 total precipitation estimates (format as in Fig. 2).
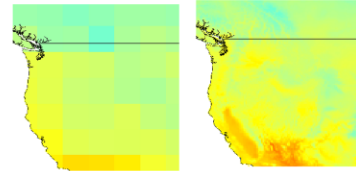
Temperature

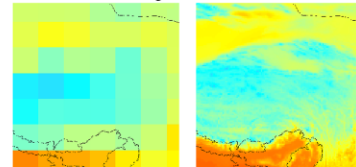2090 mean annual temperature A1B HadCM3 at native resolution (3° × 3°)

Western United States 2090 mean annual
temperature A1B HadCM3 at native resolution
(3° × 3°) on the left and regridded to
10-minute resolution on the right

Temperature (°C)

−20 −10 0   10   20 25 30 35
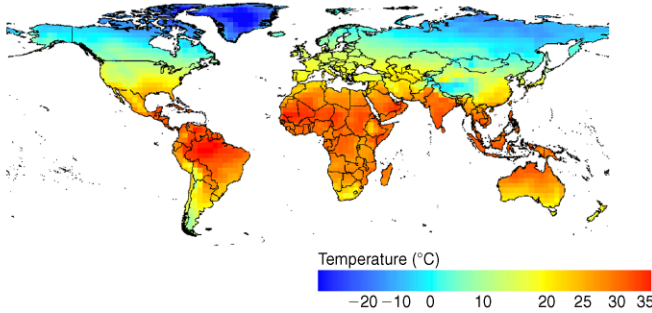
2090 mean annual temperature A1B HadCM3 regridded to 10-minute resolution
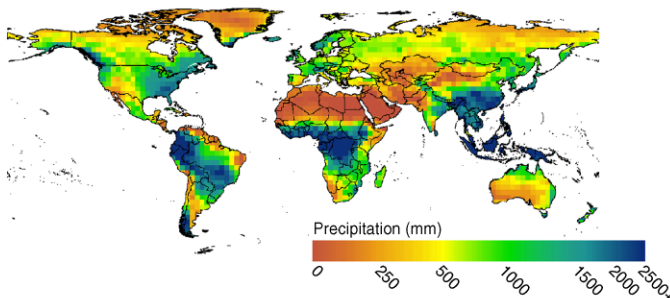
Himalayas 2090 mean annual temperature
A1B HadCM3 at native resolution (3° × 3°)
on the left and regridded to 10-minute
resolution on the right

Precipitation

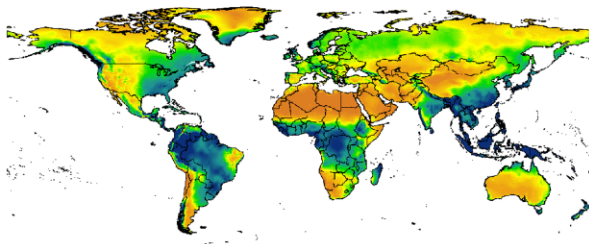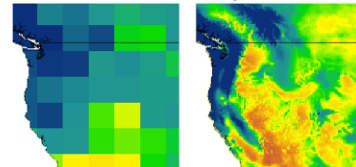2090 total annual precipitation A1B HadCM3 at native resolution (3° × 3°)

Western United States 2090 total annual
precipitation A1B HadCM3 at native resolution
(3° × 3°) on the left and regridded to
10-minute resolution on the right

Precipitation (mm)

0   250   500   1000   1500   2000   2500+

2090 total annual precipitation A1B HadCM3 regridded to 10-minute resolution

Himalayas 2090 total annual precipitation
A1B HadCM3 at native resolution (3° × 3°)
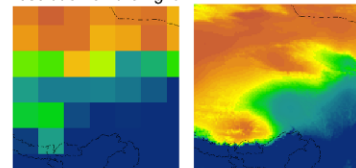on the left and regridded to 10-minute
resolution on the right

FIG. 4. These maps compare the spatial patterns of annual mean temperature and precipitation between the native grid resolution for an AOGCM and the downscaled 10-minute data sets generated here, using as an example the 2090 projections from the HadCM3 global climate model and scenario A1B (the middle CO_2-concentration scenario: 717 ppm by AD 2100). The top two global maps compare mean annual temperature at 3° × 3° vs. 10-minute grid resolution, with inset maps to the right showing the same comparisons for western United States and the Himalayas. The bottom two global maps and their corresponding inset maps make the same comparisons for total annual precipitation.

but sharp differences are apparent at regional to continental scales (Fig. 4). These differences reflect both the higher resolution of the downscaled data and the debiasing resulting from the change-factor method. To show these differences, we use as an example both the native-resolution (3° × 3°) and downscaled maps of the

2090 mean climatologies from the HadCM3 model for the A1B scenario, both globally and regionally for Himalayas and the western United States. On a global scale there is a noticeable improvement, with smoother temperature gradients, better definition of mountainous regions, and more accurate precipitation patterns in the

10-minute regridded data. The utility of high-resolution data is most obvious in mountainous regions. Regions where the change-factor debiasing substantially changes the 21st-century projections include (1) northern Eurasia, which is warmer in the downscaled maps than in the native HadCM3 maps, (2) the North American Great Plains, northern Australia, eastern Russia, and southern Africa, which are drier in the debiased maps, and (3) northeastern South America, which is wetter in the debiased maps.

In the western United States, the 10-minute regridded 2090 mean annual temperature shows much warmer temperatures in the Central Valley of California and the lowland desert of Southwest Arizona (Fig. 4). The climate of these lowland arid regions is very different from the coastal regions directly west and mountain regions to the east, yet 2090 temperatures for these regions are not discernable with the spatially coarse $3° \times 3°$ model output. The differences between the coarse-resolution and downscaled precipitation maps for the western United States are even more striking (Fig. 4: bottom). In the raw $3° \times 3°$ precipitation maps, the entire western United States has precipitation in excess of 1000 mm, whereas the downscaled maps more accurately show the spatial precipitation patterns resulting from the rain-shadow effects of the Cascade, Sierra, and Rocky Mountains.

Similarly, in the Himalayas, the 10-minute regridded temperature map depicts warmer temperatures in the river valleys that are not visible at the original resolution (Fig. 4). Precipitation patterns also differ strikingly between the 10-minute and native-resolution maps, with the former showing a very sharp precipitation gradient between the western and eastern Himalayas that is missed in the raw model output.

DISCUSSION AND CONCLUSIONS

These 10-minute debiased and downscaled climate data sets have been developed with the goal of providing conservation biologists and other climate-impact researchers the capacity for high-resolution, global-scale, ensemble projections of ecological impacts of climate change. The resulting high-resolution climate data show substantial spatial heterogeneity in all climate variables, particularly in mountainous regions, and reveal precipitation patterns not captured at the AOGCM's native resolutions, although with the caveats outlined in the *Introduction* and below. These high-resolution climatic data sets thus allow more spatially detailed projections of future species distributions and extinction risk (see Plate 1). For example, these finer-scale temperature maps may enable scientists to predict species migration to higher elevations to maintain preferred habitat. Additionally, as shown in our comparisons of the native-resolution and downscaled climate projections, the downscaled climate projections have the advantage of being corrected for systematic biases between observed and simulated

climatologies. Thus, these debiased climate projections more accurately depict future climates and can be employed for more accurate projections of species range shifts. Debiasing is particularly important for moisture-related variables, which are less robustly simulated by global climate models, yet are critical controls on species and communities, e.g., woody-plant diversity (O'Brien 1998). Finally, the reduction in grid cell size of the downscaled climate projections diminishes overestimation of suitable habitat for future species distributions (and thereby under-predicting risk of extinction) by better capturing landscape heterogeneity.

The availability of downscaled simulations from multiple models is valuable for inter-model comparisons and assessments of inter-model variability. Inter-model variability is a critical source of uncertainty to bioclimatic envelope models because their predictions of future species distribution are directly derived from the climate simulations that are used as inputs (Heikkinen et al. 2006). For example, species range projections might be highly variable for the tropics where there is large discrepancy of projected precipitation among GCMs (Kharin and Zwiers 2007, Scherrer and Baettig 2008). Identifying a single, most reliable model for regional studies is not possible (Martínez-Meyer 2005). Using multi-model ensemble means for regional studies has proven superior to using any single climate model because averaging the model projections reduces both mean errors and variance in the models (Pierce et al. 2009). Therefore, modelers use future climates derived from multiple climate models for bioclimatic envelope modeling or project species distributions using multiple climate-model inputs to assess uncertainties in the outcomes (Beaumont et al. 2007). Quantifying the uncertainties is necessary to evaluate the reliability of the model projections.

Although downscaling accessible GCMs to finer resolutions is vital for modeling climate-change impacts, there are practical constraints to GCM downscaling, and thus downscaled maps must be used critically. There are four major sources of uncertainty in the downscaled climate projections: (1) uncertainties in future greenhouse gas emissions and atmospheric composition (scenario uncertainty), (2) uncertainties in modeling the climate response (GCM uncertainty), (3) uncertainties in the observational data sets used as the basemap for the debiasing procedure (observational uncertainty), and (4) uncertainty over the validity of the assumptions underlying the change-factor approach (change-factor uncertainty). The first two are comprehensively reviewed in the IPCC AR4 report (Meehl et al. 2007*b*) and are not discussed further here, except to note that they are substantial. For example, global mean temperature predictions have an uncertainty range of several degrees Celsius, and GCMs often disagree over the direction of future precipitation trends (Meehl et al. 2007*b*).

PLATE 1. King Protea in Oudtshoorn, South Africa. Shifting range boundaries as a result of climate change have been observed for multiple species in the Cape Floristic region, a region that has already experienced a 30-year warming trend. A majority of flowering plants in the endangered and endemic fybos habitat of this region, such as *Protea cynaroides*, will lose much of their present habitat as they migrate upslope following cooler temperatures, and some species will lose all suitable habitat within their climatic range (Hannah et al. 2005). Photo credit: T. Mildenhall.

Observational uncertainty is determined by the spatial density and precision of weather- station data, which limit the accuracy and resolution of the 20th-century observational data sets and in turn limit the value added from downscaling projected climate data sets using observational data sets. Weather-station networks are particularly sparse in mountainous tropical regions, which creates a significant source of uncertainty when generating high-resolution gridded climate observational data sets for these regions. Although the spatial interpolation of temperature variables in mountainous regions can be lapse-rate corrected (Willmott and Matsuura 1995), correcting for elevational effects on interpolated precipitation variables is much more difficult. Precipitation uncertainty can be 500 mm or more in mountainous regions where station data are sparse (Hijmans et al. 2005). In general, all measured variables suffer increased interpolation errors in cold, dry and mountainous regions where station networks are sparsest (New 2002).

Downscaling methods also create uncertainties in downscaled climate data sets in part because GCMs are optimized to predict future climate at their native resolutions (Wilby et al. 2004). The two key assumptions of the change-factor approach are (1) that the relationship between macroclimates and microclimates is constant over time and (2) that model bias is constant

over time. These are assumptions of stationarity, where spatial and temporal patterns from the 20th-century observational data set are projected to a future climate period despite the possibility that climate patterns or proportion of model bias might otherwise have changed (Wilby et al. 2004, Diaz-Nieto and Wilby 2005). The change-factor approach will not capture local- to regional-scale climate changes that emerge from inter- actions between local land surfaces and radiatively driven changes in global climate. The utility of change-factor downscaling in mountainous regions likely is most limited for precipitation variables, which will be strongly influenced by local orographic effects.

There is no fixed rule about how fine resolution a climate grid can be generated from weather station networks of varying density. Fine-resolution observa- tional data sets are currently available at resolutions ranging from 30-arc-seconds to 0.5° (New et al. 2002, Hijmans et al. 2005; PRISM Climate Group, data *available online*).[6] Klausmeyer and Shaw (2009) recently used the change-factor approach to downscale GCMs from the CMIP3 multi-model data set to 2.5-minute resolution using WorldClim (Hijmans et al. 2005) temperature and precipitation as the 20th-century

---

[6] ⟨http://prism.oregonstate.edu⟩

observed data set. Klausmeyer and Shaw (2009) evaluated the errors associated with the change-factor downscaling to 2.5-minute resolution and concluded that, for temperature, errors introduced in downscaling were less than GCM uncertainties, and errors in precipitation downscaling are larger but more difficult to quantify considering the spatial and temporal uncertainty of GCMs. We have opted here to downscale to a somewhat more conservative 10-minute resolution, given the previously discussed uncertainties. However, further analysis is needed to explore the trade-offs between the value added vs. errors accumulated for downscaling from GCM model resolutions and intermittently sparse weather station networks to the increasingly fine-scale resolutions demanded by GIS-based impact assessments. Other studies of scale dependency on predictive modeling can help identify the appropriate resolution for downscaling environmental data for various forecasting models and geographic regions.

None of the uncertainties discussed here are particular to this study, but are instead a general phenomenon of climate modeling and downscaling. Thus, conservation biologists should use climate projections, downscaled or not, with appropriate caution. Discretion is necessary when using downscaled climate projections since downscaling GCMs to the finest achievable resolution might not be appropriate for some modeling applications and may produce misleading results. For example, a recent application of downscaled data for species modeling indicates no improvements of model predictions using downscaled data in montane regions because downscaled macro-scale climate models are biased against cold, high-elevation habitats (Trivedi et al. 2008). This bias results in an overestimate of a species' tolerance range for suitable habitat and yields model predictions with inflated future species distributions (Trivedi et al. 2008). Nonetheless, the urgent need for downscaled climate data sets is undeniable, given the threats posed to biodiversity by climate change (Midgley et al. 2002, Pearson and Dawson 2003, Thomas et al. 2004, Thuiller et al. 2005) and the fact that GCM simulations at native resolution are simply too coarse to be used for modeling the heterogeneous distribution of species and communities across landscapes. Our downscaled, global, 21st-century climate scenarios from IPCC AR4 accommodate the immediate demand for fine-resolution climate projections and enable and enhance efforts to conserve biodiversity in the face of large and rapid climate change.

Literature Cited

Araújo, M. B., and A. Guisan. 2006. Five (or so) challenges for species distribution modelling. Journal of Biogeography 33: 1677–1688.

Beaumont, L. J., A. J. Pitman, M. Poulsen, and L. Hughes. 2007. Where will species go? Incorporating new advances in climate modeling into projections of species distributions. Global Change Biology 13:1368–1385.

Benestad, R. E., L. Hanssen-Bauer, and E. J. Førland. 2007. An evaluation of statistical models for downscaling precipitation and their ability to capture long-term trends. International Journal of Climatology 27:649–665.

de Boor, C. 1978. A practical guide to splines. Springer-Verlag, New York, New York, USA.

Diaz-Nieto, J., and R. L. Wilby. 2005. A comparison of statistical downscaling and climate change factor methods: Impacts on low flows in the River Thames, United Kingdom. Climatic Change 69:245–268.

Díez, E., C. Primo, J. A. García-Moya, J. M. Gutiérrez, and B. Orfila. 2005. Statistical and dynamical downscaling of precipitation over Spain from DEMETER seasonal forecast. Tellus 57A:409–423.

Diffenbaugh, N. S., F. Giorgi, and J. S. Pal. 2008. Climate change hotspots in the United States. Geophysical Research Letters 35:L16709.

Evans, J. 2008. MEXNC, SNCTOOLS, and the NetCDF Toolbox. ⟨http://mexcdf.sourceforge.net⟩

Fowler, H. J., S. Blenkinsop, and C. Tebaldi. 2007. Linking climate change modeling to impacts studies: recent advances in downscaling techniques for hydrological modeling. International Journal of Climatology 27:1547–1578.

Giorgi, F., and N. Diffenbaugh. 2008. Developing regional climate change scenarios for the use in assessment of effects on human health and disease. Climate Research 36:141–151.

Hanna, L., G. Midgley, G. Hughs, and B. Bomhard. 2005. The view from the Cape: extinction risk, protected areas, and climate change. BioScience 55:231–242.

Hayhoe, K., et al. 2004. Emissions pathways, climate change, and impacts on California. Proceedings of the National Academy of Sciences (USA) 101:12422–12427.

Heikkinen, R. K., M. Luoto, M. B. Araújo, R. Virkkala, W. Thuiller, and M. T. Sykes. 2006. Methods and uncertainties in bioclimatic envelope modeling under climate change. Progress in Physical Geography 30:751–777.

Hewitson, B. C., and R. G. Crane. 2006. Consensus between GCM climate change projections with empirical downscaling: precipitation downscaling over South Africa. International Journal of Climatology 26:1315–1337.

Hijmans, R. J., S. E. Cameron, J. L. Parra, P. G. Jones, and A. Jarvis. 2005. Very high resolution interpolated climate surfaces for global land areas. International Journal of Climatology 25:1965–1978.

IPCC [Intergovernmental Panel on Climate Change]. 2007. Climate change 2007: synthesis report. Contribution of working groups I, II, and III to the Fourth Assessment Report of the Intergovernmental Panel on Climate Change [Core Writing Team, R. K. Pachauri, and A. Reisinger, editors]. IPCC, Geneva, Switzerland.

Kharin, V. V., and F. W. Zwiers. 2007. Changes in temperature and precipitation extremes in the IPCC ensemble of Global couples model simulations. Journal of Climate 20:1419–1444.

Kittel, T. G. F., N. A. Rosenbloom, T. H. Painter, and D. S. Schimel, VEMAP Modeling Participants. 1995. The VEMAP integrated database for modeling United States ecosystem/ vegetation sensitivity to climate change. Journal of Biogeography 22:857–862.

Klausmeyer, K. R., and M. R. Shaw. 2009. Climate change, habitat loss, protected areas and the climate adaptation potential of species in Mediterranean ecosystems worldwide. PLoS One 4(7):e6392.

Kremen, C., et al. 2008. Aligning conservation priorities across taxa in Madagascar with high-resolution planning tools. Science 320:222–226.

Malcolm, J. R., A. Markham, R. P. Neilson, and M. Garaci. 2002. Estimated migration rates under scenarios of global climate change. Journal of Biogeography 29:825–849.

Martínez-Meyer, E. 2005. Climate change and biodiversity: some consideration in forecasting shifts in species' potential distributions. Biodiversity Informatics 2:42–55.

MATLAB. 2007. Version r2007b. The Mathworks, Natick, Massachusetts, USA.

Meehl, G. A., C. Covey, T. Delworth, M. Latif, B. McAvaney, J. B. F. Mitchell, R. J. Stouffer, and K. E. Taylor. 2007a. The WCRP CMIP3 multi-model dataset: a new era in climate change research. Bulletin of the American Meteorological Society 88:1383–1394.

Meehl, G. A., et al. 2007b. Global climate projections. Pages 747–845 in S. Solomon, D. Qin, M. Manning, Z. Chen, M. Marquis, K. B. Averyt, M. Tignor, and H. L. Miller, editors. Climate change 2007: the physical science basis. Contribution of Working Group I to the Fourth Assessment Report of the Intergovernmental Panel on Climate Change. Cambridge University Press, Cambridge, UK.

Midgley, G. F., L. Hannah, M. C. Rutherford, and L. W. Powrie. 2002. Assessing the vulnerability of species richness to anthropogenic climate change in a biodiversity hotspot. Global Ecology and Biogeography 11:445–451.

Morin, X., and M. L. Lechowicz. 2008. Contemporary perspectives on the niche that can improve models of species range shifts under climate change. Biology Letters 4:573–576.

Nakicenovic, N., and R. Swart, editors. 2000. Emission scenarios: a special report of Working Group III of the Intergovernmental Panel on Climate Change. Cambridge University Press, Cambridge, UK.

New, M., D. Lister, M. Hulme, and I. Makin. 2002. A high-resolution data set of surface climate over global land areas. Climate Research 21:1–25.

O'Brien, E. M. 1998. Water-energy dynamics, climate, and prediction of woody plant species richness: an interim general model. Journal of Biogeography 25:379–398.

Pearson, R. G., and T. P. Dawson. 2003. Predicting the impacts of climate change on the distribution of species: Are bioclimate envelope models useful? Global Ecology and Biogeography 12:361–371.

Pierce, D. W., T. P. Barnette, B. D. Santer, and P. J. Gleckler. 2009. Selecting global climate models for regional climate change studies. Proceedings of the National Academy of Sciences (USA) 106:8441–8446.

Randall, D. A., et al. 2007. Climate models and their evaluation. Pages 589–662 in S. Solomon, D. Qin, M. Manning, Z. Chen, M. Marquis, K. B. Averyt, M. Tignor, and H. L. Miller, editors. Climate change 2007: the physical science basis. Contribution of Working Group I to the Fourth Assessment Report of the Intergovernmental Panel on Climate Change. Cambridge University Press, Cambridge, UK.

Salathé, P., Jr., P. W. Mote, and M. W. Wiley. 2007. Review of scenario selection and downscaling methods for the assessment of climate change impacts on hydrology in the United States pacific northwest. International Journal of Climatology 27:1611–1621.

Scherrer, S. C., and M. B. Baettig. 2008. Changes and inter-model spread in 21st century scenarios for temperature and precipitation extremes as seen with the climate change index (CCI). Environmental Research Letters 3:1–8.

Shongwe, M. E., W. A. Landman, and S. J. Mason. 2006. Performance of recalibration systems for GCM forecasts for southern Africa. International Journal of Climatology 26:1567–1585.

Spak, S., T. Holloway, B. Lynn, and R. Goldberg. 2007. A comparison of statistical and dynamical downscaling for surface temperature in North America. Journal of Geophysical Research 112:1–37.

Thomas, C. D., et al. 2004. Extinction risk from climate change. Nature 247:145–148.

Thuiller, W., S. Lavorel, M. B. Araújo, M. T. Sykes, and I. C. Prentice. 2005. Climate change threats to plant diversity in Europe. Proceedings of the National Academy of Sciences (USA) 102:8245–8250.

Trivedi, M. R., P. M. Berry, M. D. Morecroft, and T. P. Dawson. 2008. Spatial scale affects bioclimate model projections of climate change impacts on mountain plants. Global Change Biology 14:1089–1103.

UCAR [University Corporation for Atmospheric Research]. 2002. Earth Systems Grid [all rights reserved]. University Corporation for Atmospheric Research, Boulder, Colorado, USA. ⟨http://www.earthsystemgrid.org⟩

WDPA [World Database on Protected Areas]. 2006. 2006 World Database on Protected Areas. [CD-ROM.] IUCN World Commission on Protected Areas, UNEP World Conservation Monitoring Centre, Washington, D.C., USA.

Wilby, R. L., S. P. Charles, E. Zorita, B. Timbal, P. Whetton, and L. O. Mearns. 2004. Guidelines for use of climate scenarios developed from statistical downscaling methods. IPCC Task Group on data and scenario support for Impact and Climate Analysis (TGICA). ⟨http://ipcc-ddc.cru.uea.ac.uk/guidelines/dgm_no2_v1_09_2004.pdf⟩

Wilby, R. L., T. M. L. Wigley, D. Conway, P. D. Jones, B. C. Hewitson, J. Main, and D. S. Wilks. 1998. Statistical downscaling of general circulation model output: a comparison of methods. Water Resources Research 34:2995–3008.

Willmott, C. J., and K. Matsuura. 1995. Smart interpolation of annually averaged air temperature in the United States. Journal of Applied Meteorology 34:2577–2586.

Zhang, X. C. 2006. Spatial downscaling of global climate model output for site-specific assessment of crop production and soil erosion. Agricultural and Forest Meteorology 135:215–229.